Development of Tunable Ka-band Filters

Final Report

Ben Lacroix, Stanis Courreges, Yuan Li, Carlos Donado and John Papapolymerou

School of Electrical and Computer Engineering
Georgia Institute of Technology
Atlanta, GA 30332

Introduction/Summary

Georgia Tech has designed several filters operating in Ka-band. These filters are built on Sapphire and use integrated BST thin films as tuning elements. The fabrication is conducted by nGimat, Inc. Four different approaches are presented in this report.

The first filter is a 3-pole filter based on a CPW (Coplanar Waveguide) topology and includes 6 BST capacitors. It is built on a Sapphire substrate and tunes from 29 to 34 GHz (17%). The fractional bandwidth is about 10-12%. Insertion loss of only 2.5 dB is measured when the BST capacitors are biased with 30 V.

The second CPW filter consists of two resonators whose physical/electrical lengths can be changed by coupling each resonator with an additional piece of line which acts like a loading capacitor. Therefore, the center frequency can be tuned. The measured tuning appears to be lower than expected. Several issues are discussed.

The third filter is also based on a CPW topology, and uses 4 BST capacitors located at the end of the resonators in order to make the filter tune. This design is based on cross-coupled resonators. A trade-off between performance and tuning is discussed.

Finally, the fourth part demonstrates the design and implementation of a two-pole, Tunable Folded Waveguide Filter (TFWF) on sapphire and with tuning provided by barium strontium titanate (BST) capacitors. The filter operates in the Ka-band and has a simulated tuning range of 10% (27.72 GHz to 30.50 GHz).

Part I

3-pole tunable Ka-band filter

I. 1/ Filter design:

The design objective is a three-pole tunable BPF using BST capacitors for Ka-band with a center frequency f_0 in the Ka-band (26–40 GHz), a fractional bandwidth of around 10-12%, a return loss of 20 dB, a frequency tuning greater than 15% and a minimum OIP3 value of 15 dBm. Figure I.1 shows the three-pole coplanar tunable filter loaded with six BST capacitors (3 on each side).
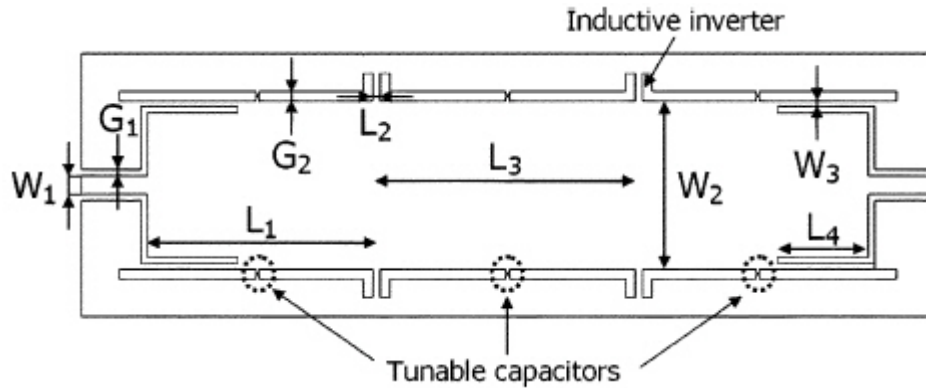

Fig. I.1. Layout of the designed three-pole tunable bandpass filter using 6 BST capacitors.

A coplanar waveguide configuration is chosen to reach the specifications of the frequency tuning and the integration of the circuit. The filter is designed by cascading three half-wavelength resonators with inductive impedance inverters. Since the electric field is maximal at the middle of the resonators, a maximum frequency shift can be achieved by loading tunable capacitors at this position. The filter is fed by original feedlines: the first part is a 50 Ω line connected to a wider short circuited line. With this feeding structure, the filter does not need bridges, and the external quality factor, Q_{ext}, can be optimized easily by modifying the length L_4, and the width W_3. It is also possible to get a wider resonator by keeping the same slot gap, which can increase the unloaded quality factor Q_0 of the filter.

The filter is made on a sapphire substrate (ε_r=10, tan δ < 0.0001 at 10 GHz). The metallization of the filter is a 2-μm thick copper. In order to meet the specifications, a coupling matrix is chosen with $R_{in} = R_{out} = 1.082$ and $k_{12} = k_{23} = 1.030$. The dimensions of the filter, the size of the feedlines and the width of the inverters are then adjusted in order to optimize the simulated S-parameters. A hybrid simulation is used to model the filter with the BST capacitors: the layout of the filter is simulated and includes internal ports at the capacitors locations. A RC lumped component model is used to represent the BST capacitor and its intrinsic loss. A capacitance ratio of 3:1 is considered (60 fF/20 fF) with a series resistance of 4 ohms. Then, the dimensions are optimized again with the loaded capacitors (Table I.1). The final size of the filter is 4560 μm x 1400 μm.

Table I.1 – Optimized dimensions of the designed 3-pole filter

Parameter	(µm)	Parameter	(µm)	Parameter	(µm)
W_1	100	L_1	1228	L_4	485
W_2	900	L_2	40	G_1	35
W_3	30	L_3	1407	G_2	50

The simulated response is shown in Figure I.2. The center frequency of the filter tunes from 28 GHz up to 34 GHz (21%) with a capacitance range of 60 to 20 fF. The fractional bandwidth ranges from 11% to 13.2% and the insertion loss, taking into account 4 series resistors, is between 3.8 dB (with C = 60 fF) and 2.8 dB (with C = 20 fF).
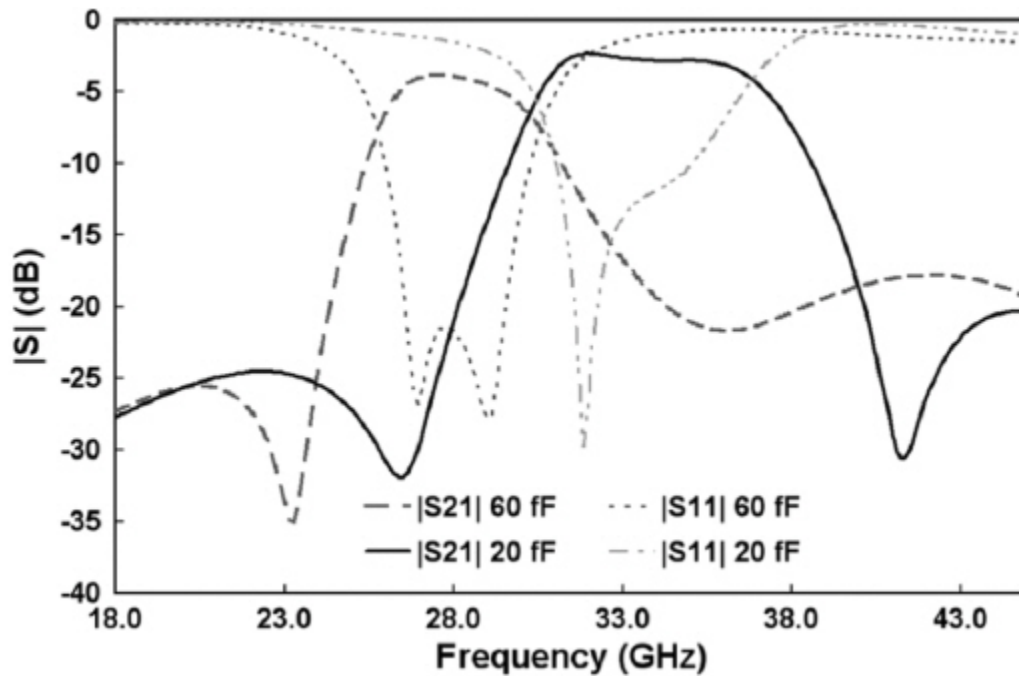
Figure I.2 – Simulated response of the designed 3-pole filter (C = 60 fF and C = 20 fF).

I. 2/ Fabrication:

The fabricated filter is presented in Figure I.3. A specific bias network has been designed to bias the BST capacitors. At 1 MHz, the capacitor values are ranging from 67 fF at 0 V to 27 fF at 30 V, resulting in a quality factor of 85 and 520 respectively.
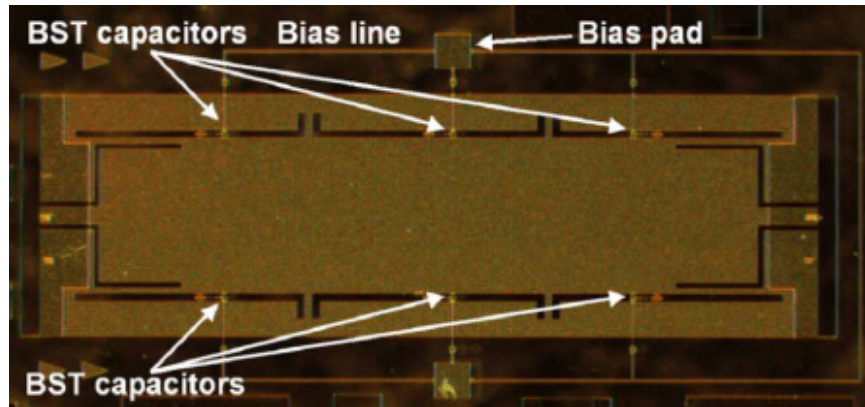
Figure I.3 – Fabricated tunable 3-pole filter.

I. 2/ Measurements:

A. S-parameters measurements

The measurements are performed using an Agilent Vector Network Analyzer 8510 C calibrated with the Short-Open-Load-Through (SOLT) standard. The bottom side of the coplanar filter (without ground plane) is fixed on foam, which has a permittivity close to 1, to imitate air. Then, the S-parameters are measured by using a probe station with bias voltages ranging from 0 V up to 30 V. Figure I.4 shows the measured return loss whereas Figure I.5 presents the measured insertion loss. The frequency tunes from 29 GHz, without bias voltage, up to 34 GHz with a voltage of 30 V. The frequency tuning is 17.2% and is close to the simulated value. The fractional bandwidth ranges from 9.5% up to 12.3%. For this technology, the filter has good insertion loss and return loss levels of 6.9-2.5 dB, and 24-13 dB, respectively, with a DC bias varying from 0 to 30 V at room temperature. This new filter, including the bias lines, has a better transmission coefficient outside the pass band at the highest frequencies: 25 dB instead of 15 dB.
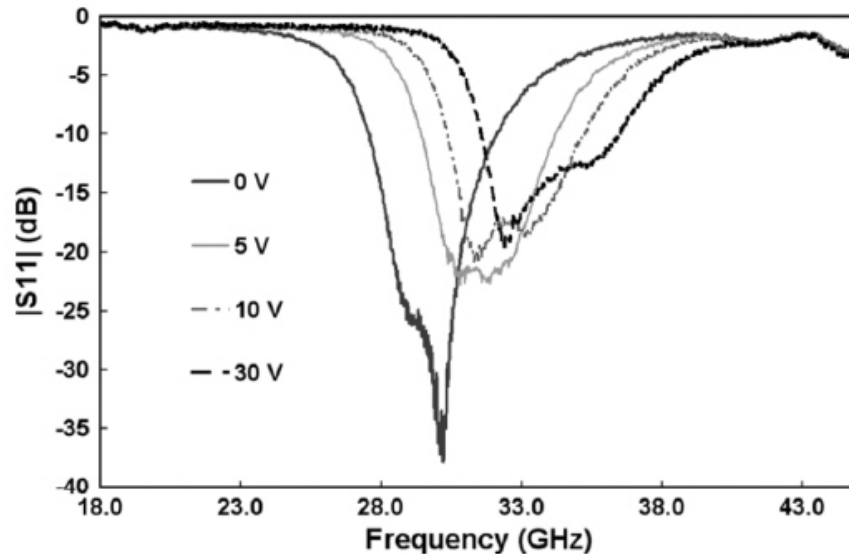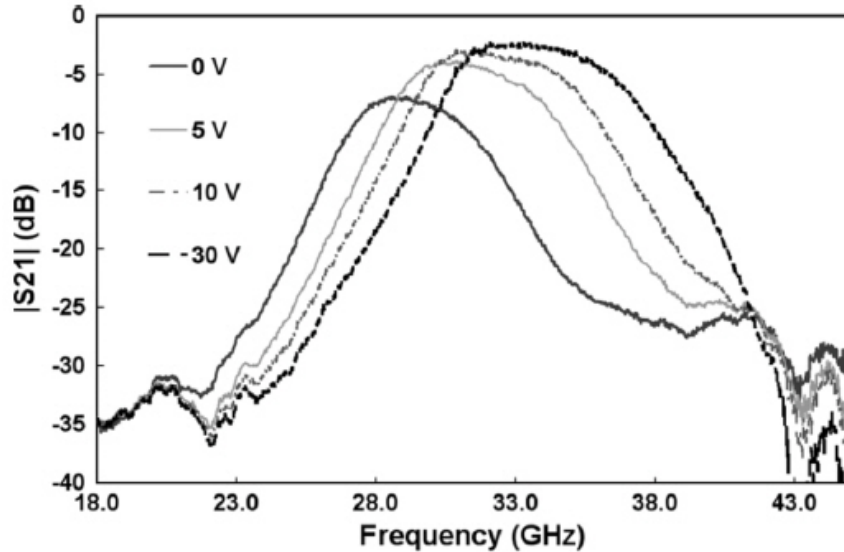

Figure I.4 – Measured return loss.

Figure I.5 – Measured insertion loss.

A. OIP3 measurements

The third order intercept point of the filter was measured on an integrated wafer-level RF measurement system capable of measuring noise, load pull, S-parameters, and intermodulation distortion up to 40 GHz without lifting the RF probes. To ensure accurate measurements, the system power level is calibrated with the reference plane located at the probe tips. This can be done by first measuring the insertion loss of the input and output RF blocks at the cable level. After an on-wafer thru-reflect-line (TRL) calibration, the insertion loss of the probes and tuners is calculated by successive one-port measurements using an open, short, and load standard at the output of each tuner. The probes are contacted to the wafer-level thru standard during these measurements. With the insertion loss known up to the probe tips, the power level can be accurately calculated using a power meter and simple addition and subtraction. Third order intercept was calculated by injecting two sinusoids at various frequency spacings. The power level of the primary tones and their third order intermodulation terms at (2f1-f2) and (2f2-f1) are then measured on a spectrum analyzer while the filter is still in the pass band of operation. The output third order intercept point can then be calculated using Eq. (1):

$$OIP_3(\text{dBm}) = \frac{\Delta P(\text{dB})}{2} + P_{out}(\text{dBm}). \qquad (1)$$

Figure II.6 presents the OIP3 results with different bias voltages: 0 V, 10 V and 30 V. The OIP3 measurements are greater than 15 dBm with frequency spacings of 100 kHz, 300 kHz and 1 MHz. These results satisfy the specifications. Also, the filter uses tunable capacitors with simple shaped electrodes. The level of OIP3 could be improved by using other shapes of electrodes.
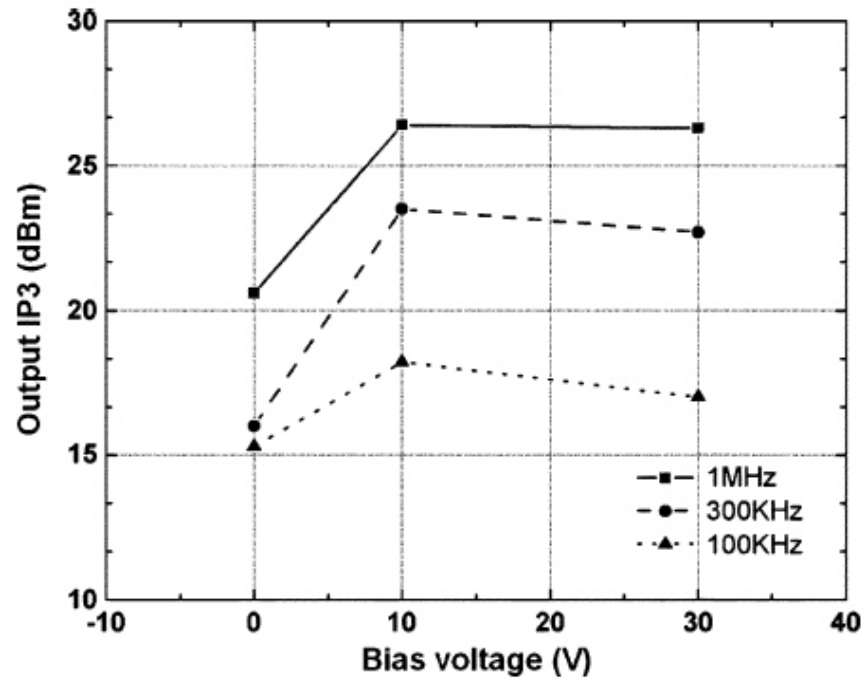
Figure II.6 – Output IP3 versus bias voltage for different frequency spacings.

Part II

2-pole tunable Ka-band filter

II. 1/ Filter design:

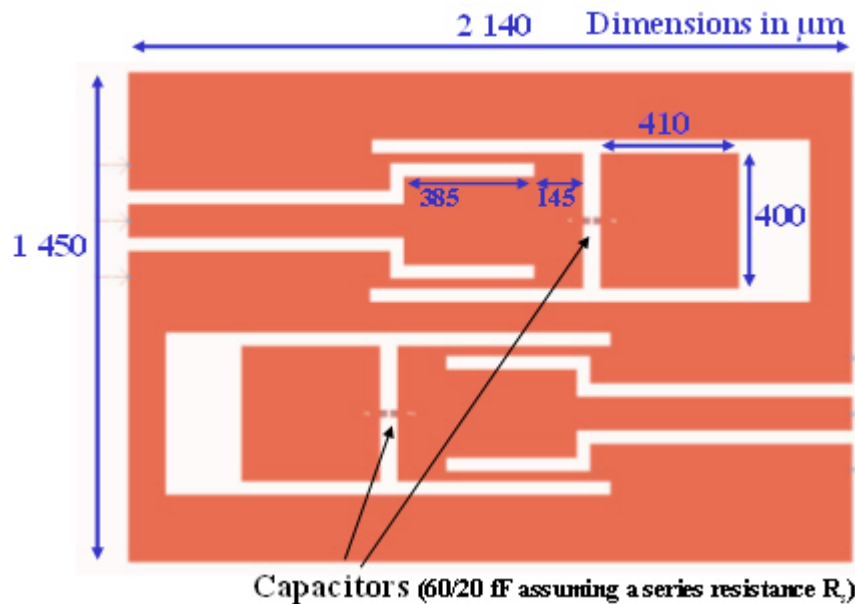The designed filter is presented in Figure. II.1.

Fig. II.1. Layout of the designed two-pole tunable bandpass filter operating in Ka-band.

This filter consists of two resonators whose electrical lengths can be changed by tuning the BST capacitor. The rectangular pieces (410 um x 400 um) act like loading capacitors or an extension of the resonators. It could be seen as a change of the physical length if the BST capacitor was an ideal switch (in that case, there would be only two states). The feedlines are similar to the ones used for the 3-pole filter presented in Section I. The dimensions of the feedlines as well as that of the resonators and the additional parts are optimized in order to get good insertion loss and return loss levels. As in the previous Section, a lumped capacitor with a series resistance is used to model the BST capacitor: since the resistance value of the BST capacitor might be high at the operating frequency range, simulations with R = 4 ohms and R = 20 ohms have been performed in order to make sure that the insertion loss can still satisfy the specifications. The capacitor value tunes from 60 fF to 20 fF. Figures II.2 and II.3 present the simulated results for R=4/20 ohms, respectively.
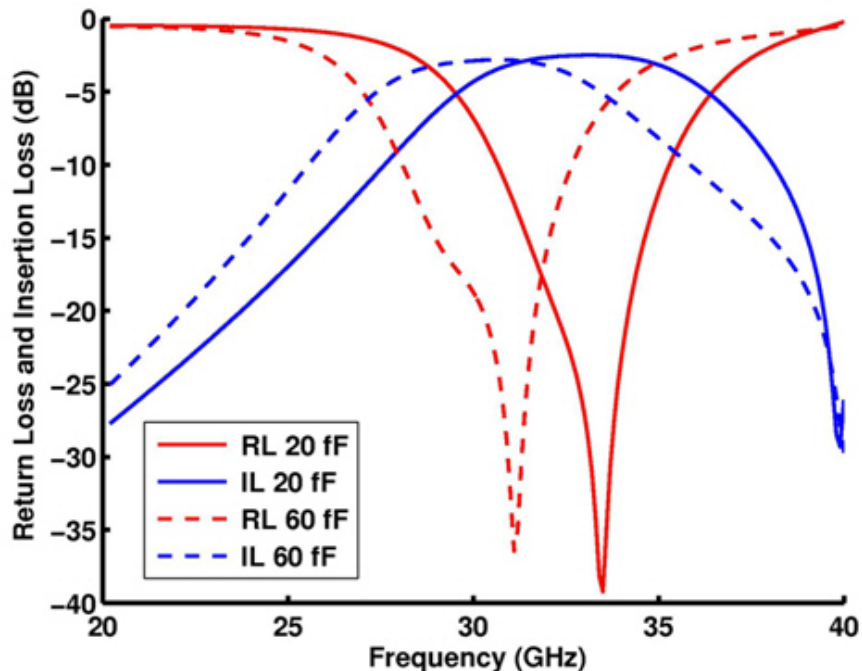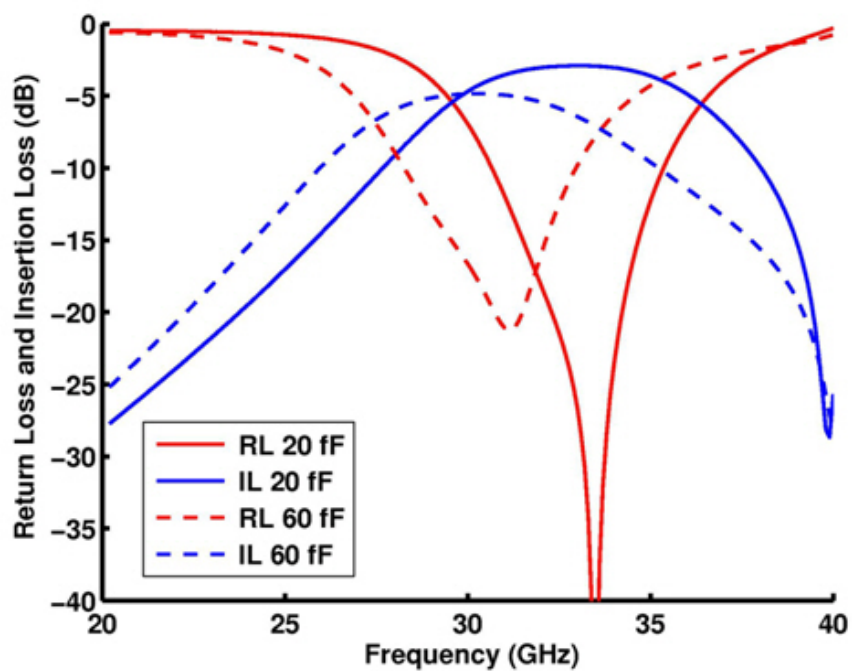
Figure II.2 – Simulated S parameters with R = 4 ohms.

Figure II.3 – Simulated S parameters with R = 20 ohms.

In both cases, the center frequency tunes from 30.4 GHz up to 33 GHz, resulting in a tuning of 7.9%. The 3-dB fractional bandwidth is about 22-23%. When a series resistance of 4 ohms is assumed, insertion loss varies from only 2.83 dB to 2.5 dB from 30.4 to 33 GHz. Even assuming a high series resistance of 20 ohms, it will change from 4.85 dB to 2.91dB (from 30.4 to 33 GHz) which is very satisfying at these frequencies.

II. 2/ Measurements:

The filter is fabricated on a sapphire substrate with a similar process as the filter presented in Section I. The filter performance is measured after an SOLT calibration is performed. However, the response (insertion loss shape) did not look like expected due to a parasitic resonance (around 32 GHz). This resonance had been attributed to parasitic modes that can occur due to the specific coplanar feedline used in this design. In order to confirm this assumption and remove this parasitic effect, bonding wires had been added in order to create a bridge between the two ground planes, at the input and output, as shown in Figure II.4.
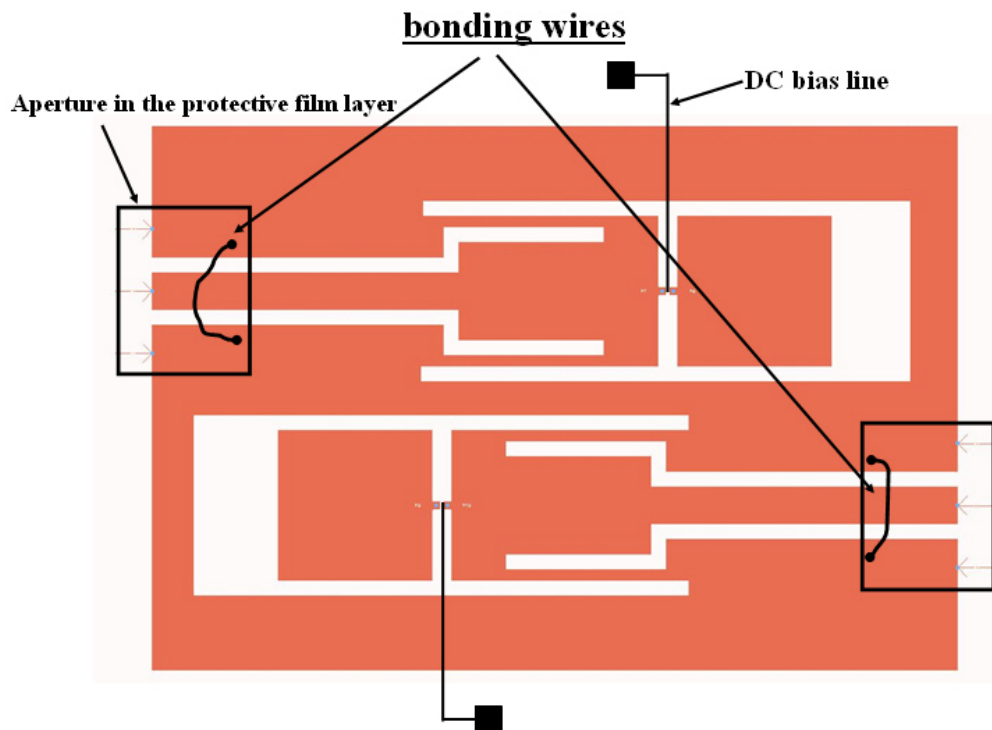

Figure II.4 – Layout of the filter with bonding wires at the input and output.

The use of bonding wires can remove the parasitic resonance. Figures II.5 and II.6 present the measured responses, without and with the bonding wires. Retro-simulations have been performed with both Momentum and HFSS, but none of these softwares were able to predict this effect. Figure II.7 and II.8 compares the simulated response to the measured one. Figure II.9 and II.10 present the simulated response with HFSS for C = 60 fF and C = 20 fF.
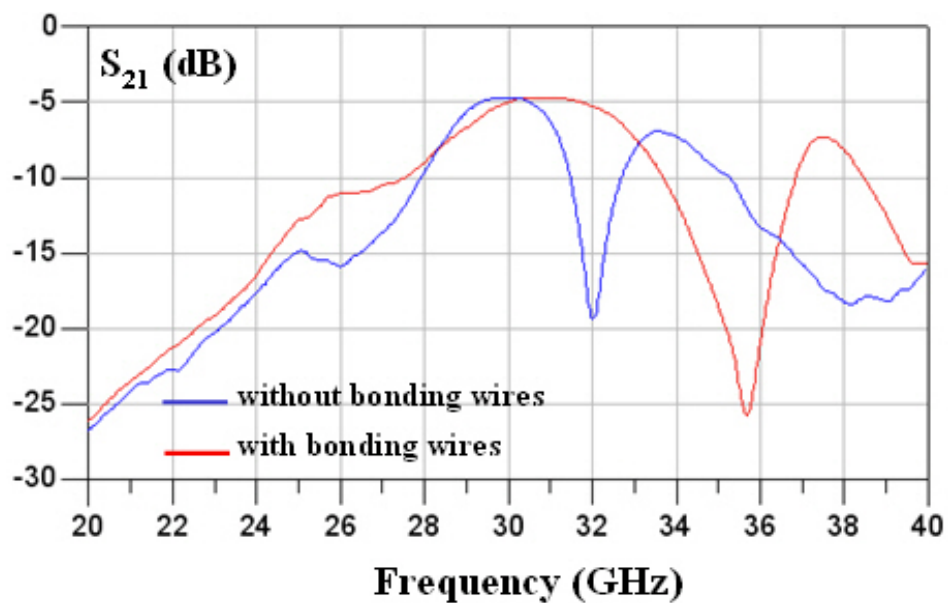
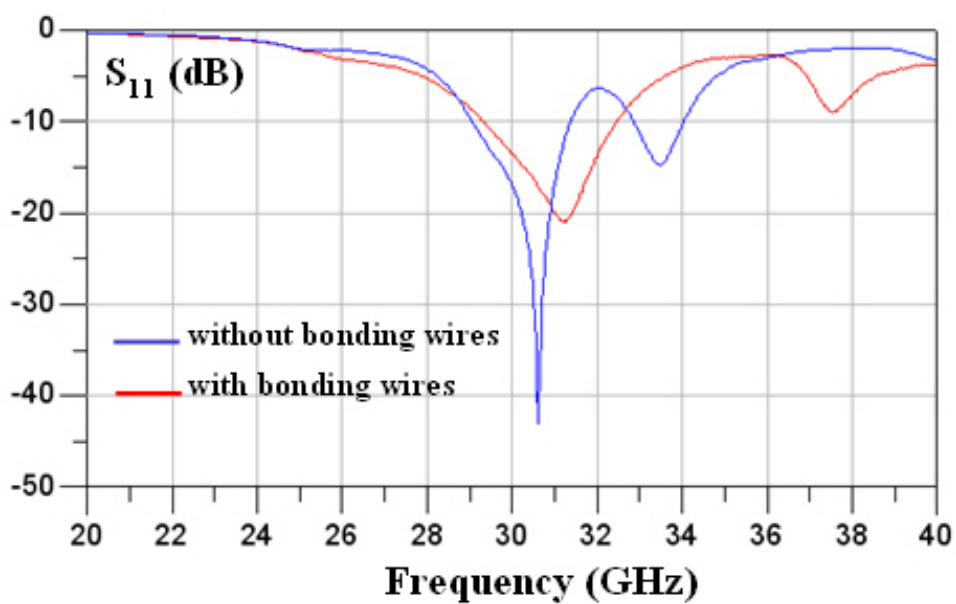Figure II.5 – Measured insertion loss without and with bonding wires.

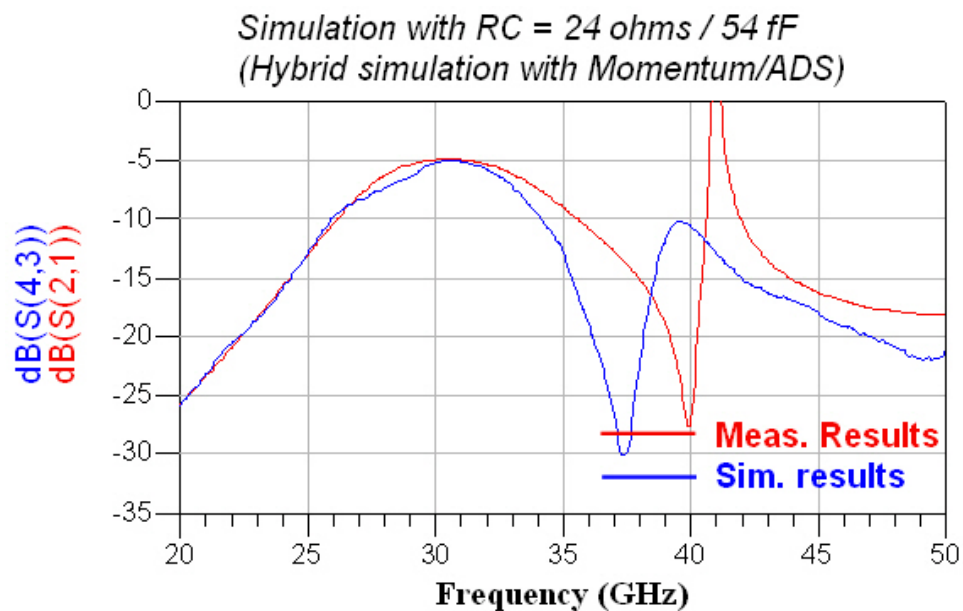Figure II.6 – Measured return loss without and with bonding wires.

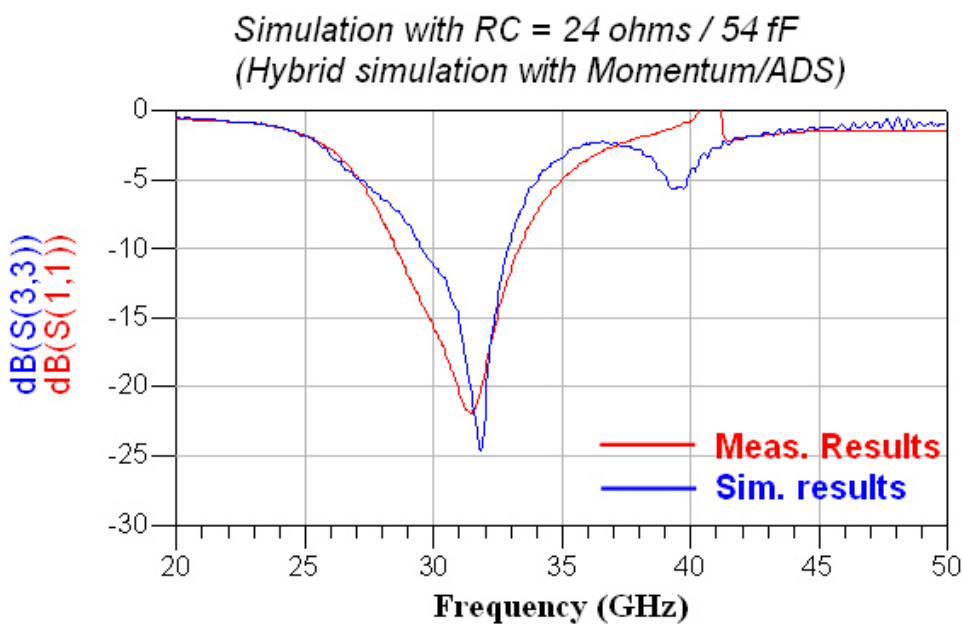Figure II.7 – Measured insertion loss compared to the simulated response.

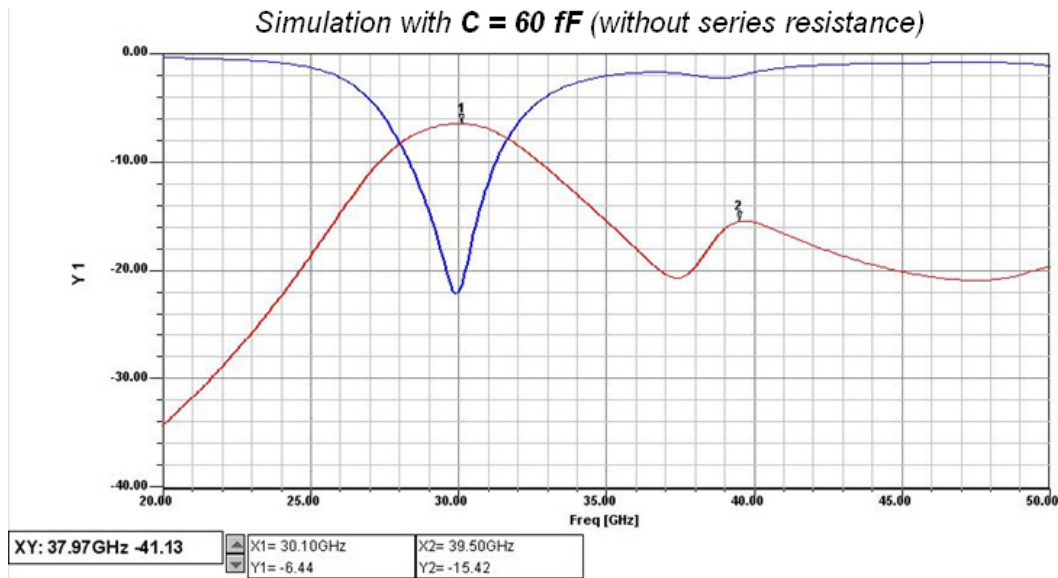Figure II.8 – Measured return loss compared to the simulated response.
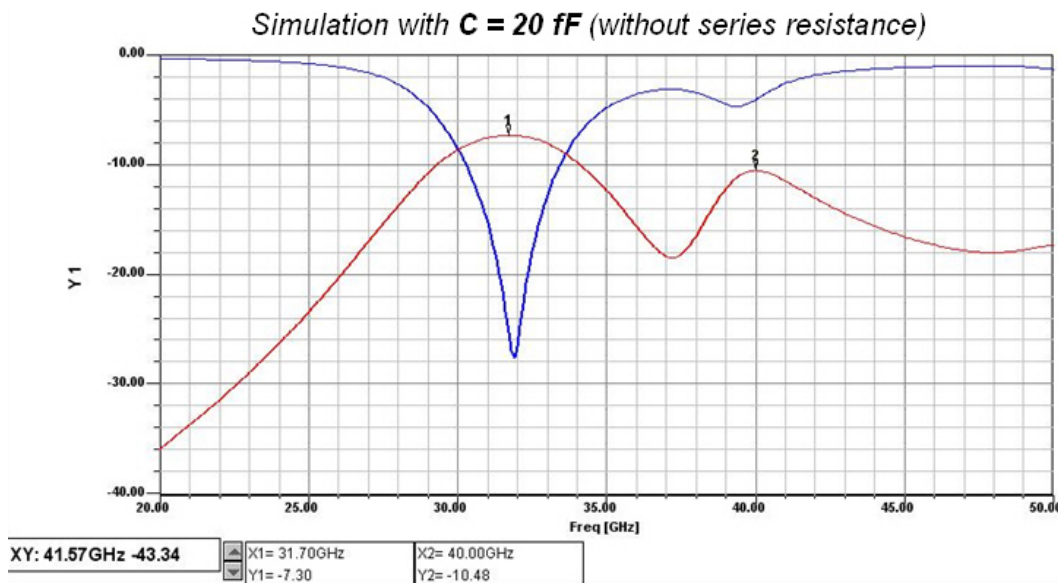
Figure II.9 – Simulated response with HFSS (C = 60 fF).

Figure II.10 – Simulated response with HFSS (C = 20 fF).

Several samples have been fabricated and tested. Two filters per sample are fabricated with 2 different biasing networks. However, it appears that for one of them, only one capacitor is working. Also, the film does not seem to handle a lot of voltage on this topology. It has been seen several times that the film broke out at only 10-20 V. When it tunes, the response does not seem to tune that much, especially the insertion loss. The tuning is very poor. This problem could be due to the quality of the film and the topology of the filter. A typical tuning achieved with the biasing of only one capacitor is presented in Figure II.11.
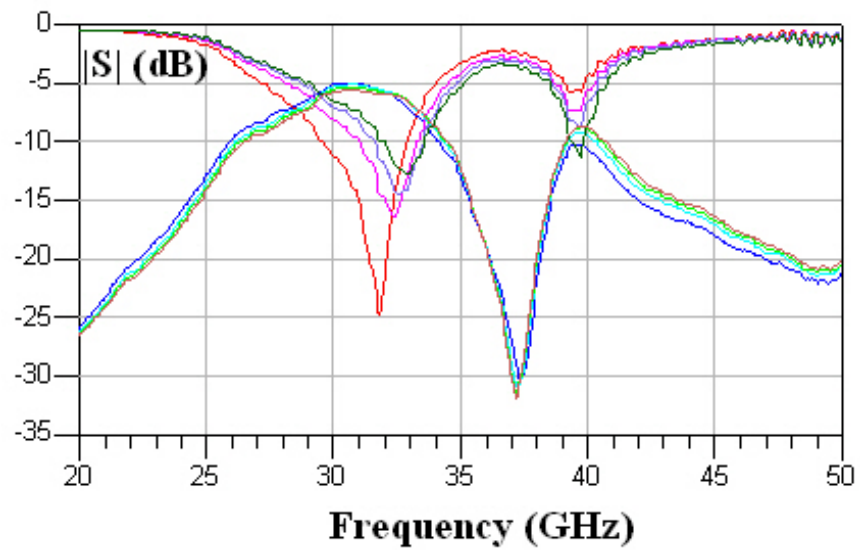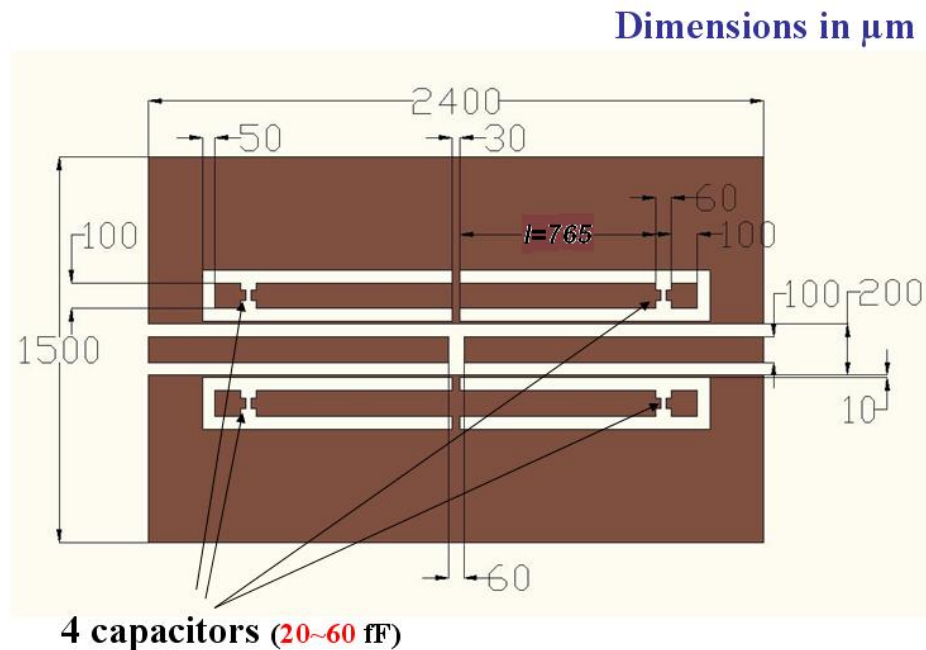
Figure II.11 – Example of "poor" tuning achieved by biasing one capacitor.

Part III

Tunable filter based on cross-coupled resonators

III. 1/ Filter design:

This Ka-band tunable bandpass filter is composed of four CPW cross-coupled quarter-wavelength resonators, which are loaded with BST thin film varactors located at the end of the resonators, as shown in Figure III.1.

Figure III.1 – Cross-coupled resonators filter.

This structure shows a quasi-elliptical band pass function. It exhibits good performance including low insertion loss in its passband and high out-of-band rejection level in both lower and upper stopbands. Furthermore, there are also two transmission zeros in its stopband and their position may be controlled by adjusting the coupling between two resonators. By changing the value of the loaded BST thin film varactors, the electrical length of the resonators can be varied, and therefore the center frequency is tuned.

The whole circuit is designed on a 430-μm thick sapphire substrate (ε_r=10). The copper metallization of the filter is 2-μm thick. The tunable capacitors range from 60 fF to 20 fF, resulting in a ratio of 3:1.

III. 1/ Simulated results:

The dimensions of a filter with relative good performance were optimized. The key factor affecting the performance of this reconfigurable filter is the location of BST thin film varactors. Decreasing the distance l between the BST thin film varactors and the center ground line (Figure III.1) will increase the tuning, but worsen the insertion/return

loss, and vice-versa. The designed filter represents a trade-off between the tuning that can be achieved and the magnitude performance. The intrinsic loss of the BST thin film varactors, which can be represented by a series resistor R, is theoretically proportional to the frequency. Working in Ka-band, this other key factor must be considered. After optimization, when $l = 765$ µm and $R = 4$ ohms, the center frequency tunes from 33 to 34.4 GHz (4.2% tuning) when the capacitance value C varies from 60 to 20 fF. The 3-dB fractional bandwidth ranges from 8.8% to 9.3%. The insertion loss changes from 4.83 dB to 4.42 dB. The simulation results are shown in Figure III.2. When R is increased to 20 ohms, the insertion loss increases to 6.41 dB and 5.07 dB at 33 GHz and 34.4 GHz, respectively, as shown in Figure III.3.
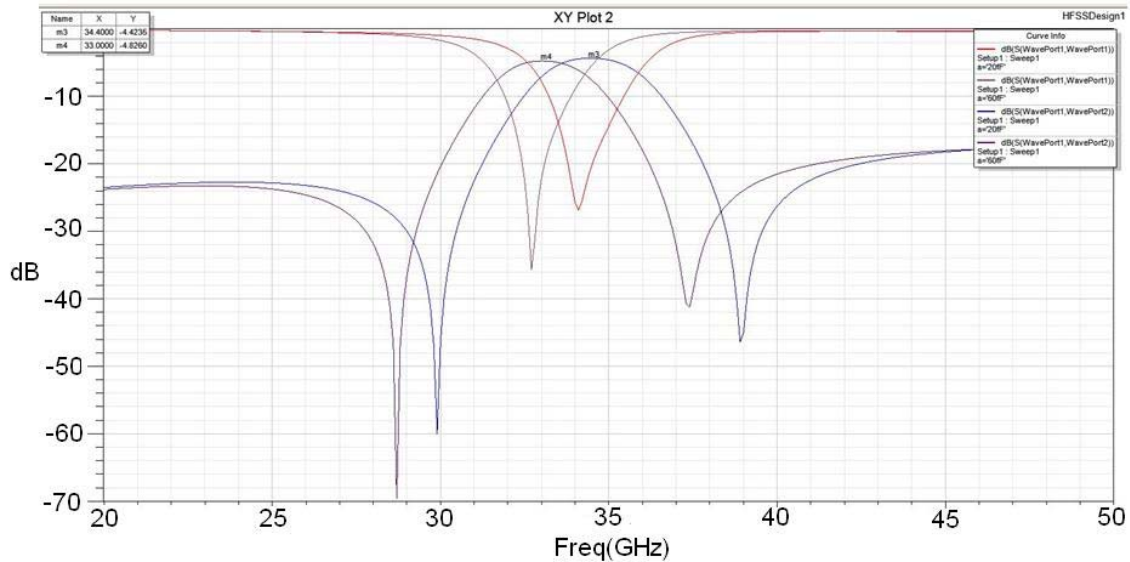

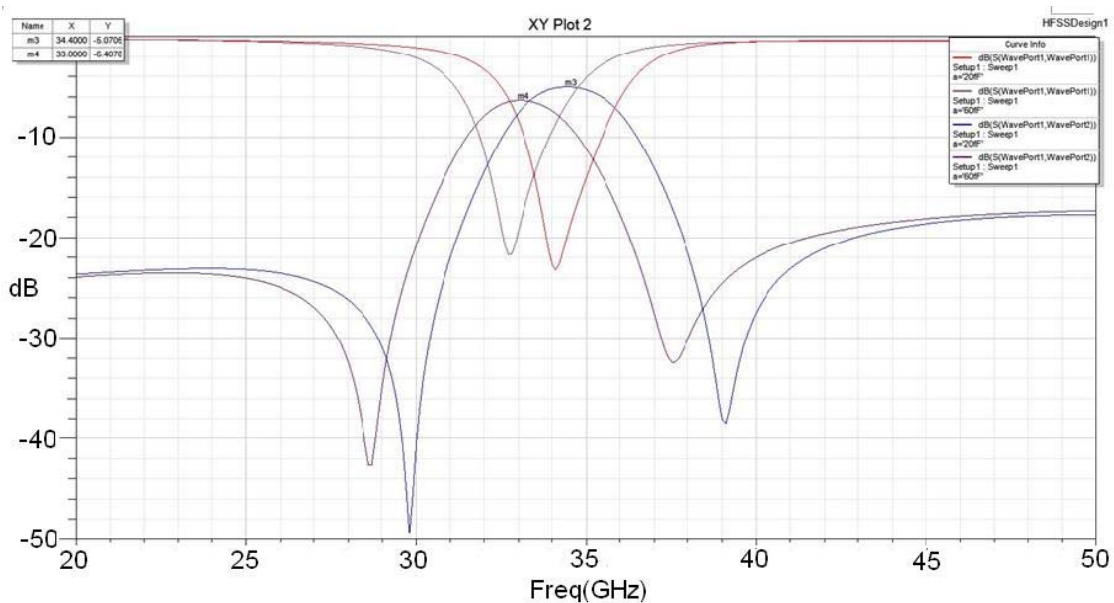Figure III.2 – Simulated response with R = 4 ohms (l = 765 µm).

Figure III.3 – Simulated response with R = 20 ohms (l = 765 µm).

In order to get a better tuning, *l* can be modified. For $l = 665\mu m$ and $R = 4$ ohms, the center frequency tunes from 33 to 36.9GHz, resulting in a tuning of 11.2%, when C changes from 60 to 20 fF, as shown in Figure III.4. The insertion loss is about 5.74 dB at 33 GHz and 4.61 dB at 36.9GHz. However, assuming a high series resistance of 20 ohms, the insertion loss deteriorates a lot: 10.1 dB at 33GHz and 6.04 dB at 36.9 GHz, as shown in Figure III.5.
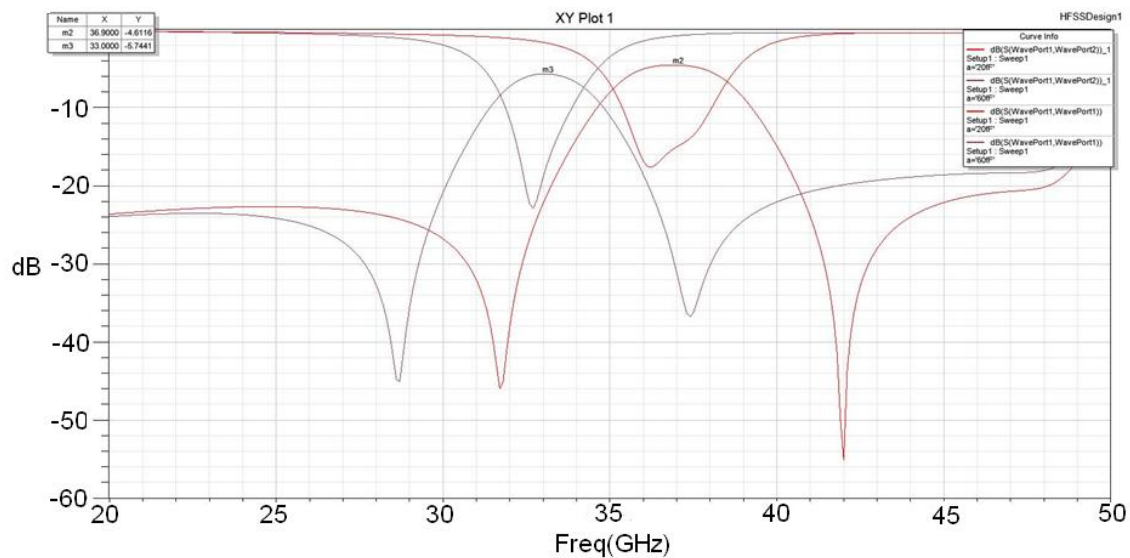

Figure III.4 – Simulated response with R = 4 ohms (l = 665 μm).

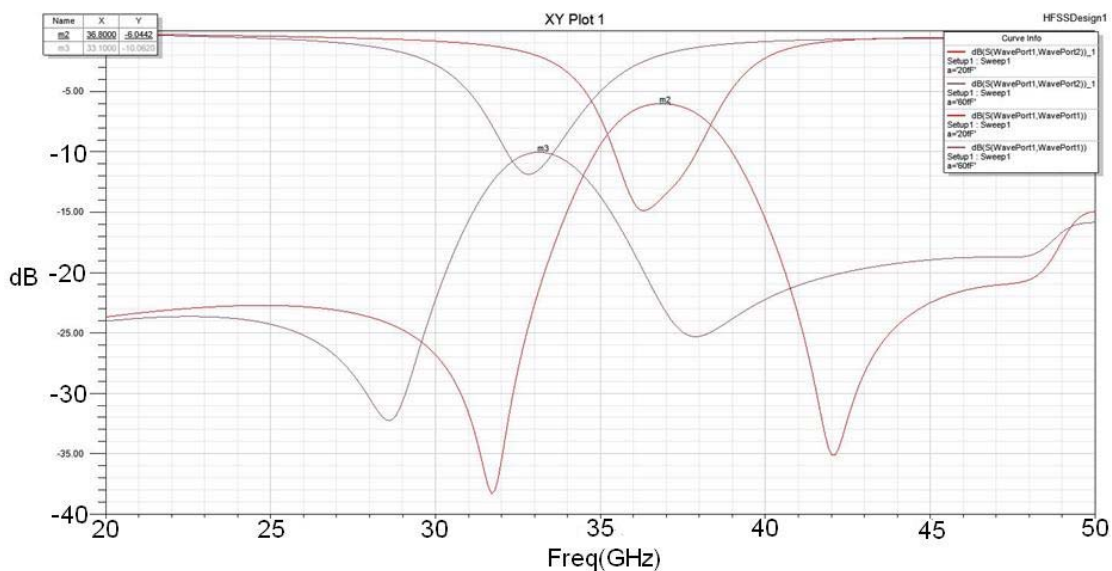Figure III.5 – Simulated response with R = 20 ohms (l = 665 μm).

Part IV

Development of a tunable, folded-waveguide filter in the Ka-band

IV. 1/ Folded Waveguide: Principle of operation and Design:

The basic operation of a folded waveguide is extensively explained in [1] and in [2]. In a folded waveguide, the fundamental TE_{10} mode of a rectangular waveguide (Figure IV.1) is "folded" around the longitudinal axis running across the center of one of the sides indicated with dimension *2a* (Figure IV.1) of the waveguide. Therefore, the folding process reduces the footprint area of the filter by half as the longer side of the rectangular waveguide cross-section is reduced from *2a* to *a* (Figure IV.2). By providing a slot aperture of width *w* across the axis where the folding is performed, it is possible to properly develop the TE_{10} mode in a "folded" fashion, as shown in Figure IV.2.
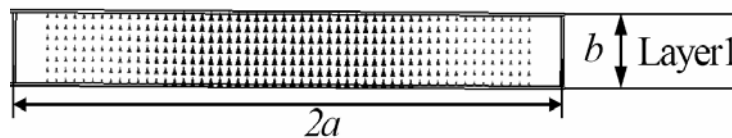

Figure IV.1 - Rectangular waveguide cross-section showing the electric field distribution of the TE_{10} mode (Fig. IV.1 from [2]).
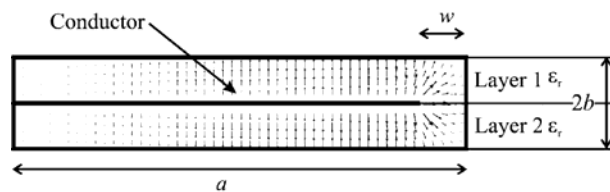

Figure IV.2 - Folded rectangular waveguide cross-section showing the electric field distribution for the "folded" TE_{10} mode (Fig. IV.2 from [1]).

In [1], designs rules are also presented to obtain the dimensions of the waveguide for folded operation. Fixing the substrate height (*b=430 μm*) and by using *b/a=0.4* (as suggested in [1]), we find that *a=1075 μm*. In addition, we see that *w/a=0.05* so the width of the slot that allows the folded operation is *a=53.75 μm*. Next, we proceed to verify whether the bandwidth of the folded waveguide is *not* less than the rectangular waveguide by verifying that *2w/a < b/a*, which for our case *0.1 < 0.4* properly holds.
To verify that the design rules chosen correctly apply for our application and materials, we proceeded to simulate using HFSS [3] the folded waveguide using a sapphire substrate with $ε_r=10.0$. We see that the waveguide operation is substantially above the cut-off frequency as shown in the propagation constant plot in
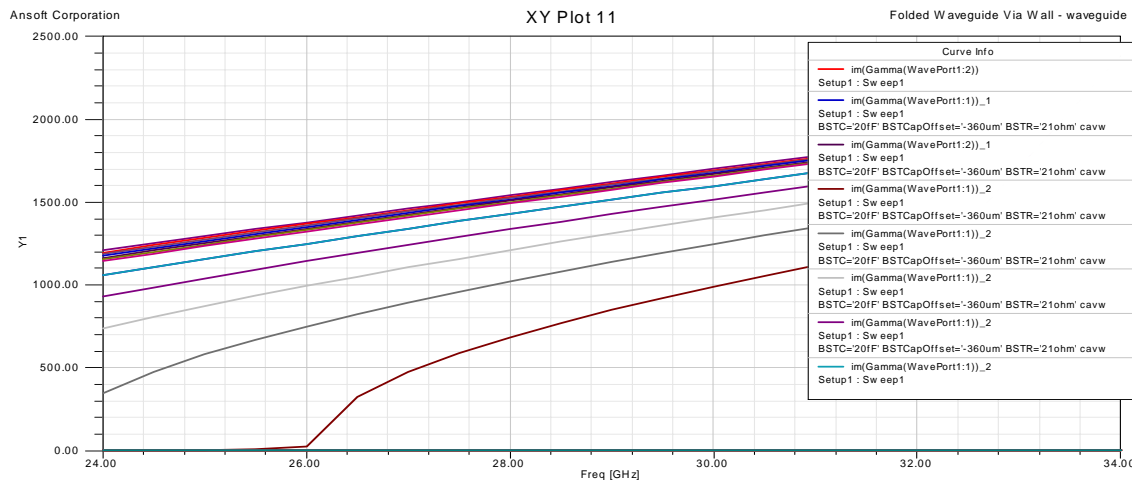Figure IV.3 (all distances simulated are above *a=1075 μm*).

Figure IV.3 - Propagation constant plots showing the low cut-off frequency of the folded waveguide for different widths of the folded waveguide.

IV. 2/ Resonator design:

In this design two $\lambda_g/2$ (half the guided wavelength) resonators will be utilized to provide two poles in the pass band. An initial approximation of the $\lambda_g/2$ length is obtained with the Line Calculation tool available in [4] using a rectangular waveguide and then optimized in HFSS using a weak coupling. The low input/output coupling allows the determination a center frequency of about 32 GHz. From the optimized model we obtain that $\lambda_g/2=1500\ um$.

IV. 3/ The 2-pole filter realization:

After the $\lambda_g/2$ length has been chosen, the realization of the two-pole filter is performed by placing two $\lambda_g/2$ sections next to each other as done in [1]. Due to the high quality factor of the folded waveguide resonators, a weak coupling between the $\lambda_g/2$ sections is provided by extending and optimizing the length of the inter-resonator coupling section in the "Layout" layer shown in
Figure IV.4.a.

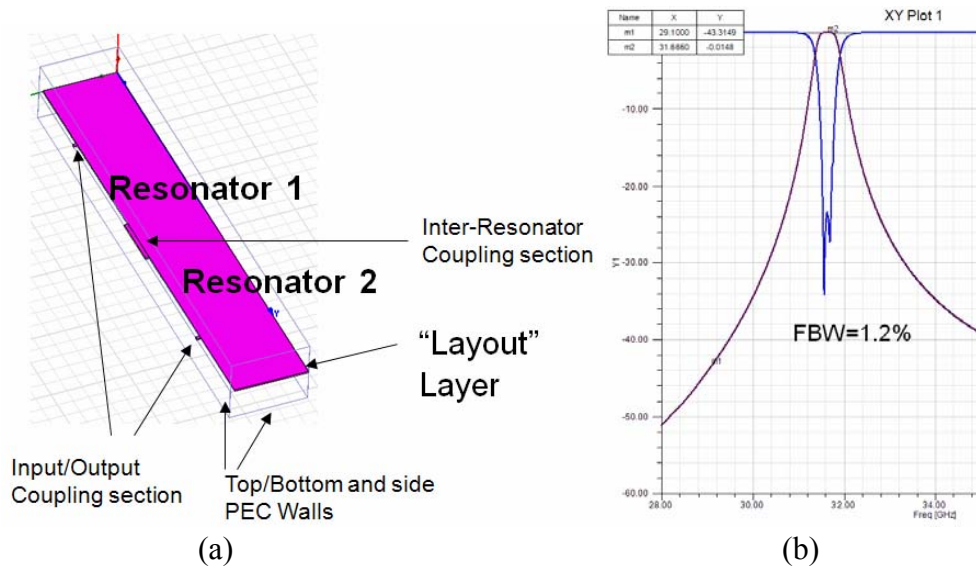(a)   (b)

Figure IV.4 – (a) Ideal realization of the two-pole filter using two $\lambda_g/2$ sections,
(b) Simulated S-parameter response of the folded waveguide filter with S_{11} in blue and
S_{21} in maroon.

The input/output and inter-resonator coupling sections were optimized using HFSS to obtain the S-parameter response in
Figure IV.4b. A Perfect Electric Conductor (PEC) metallization was utilized to obtain the shown response.
Through the simulations we could observe that the lowest reflected signal level in the pass band (S_{11},
Figure IV.4.b) is achieved by shrinking as much as possible the length of the coupling section. Consequently, the level of S_{11} is limited by the minimum line width that can be patterned on the metallization layer of the circuit.

IV. 4/ Realization of the Vertical Walls of the Folded Waveguide:

Undoubtedly, the fabrication of the vertical walls of the folded waveguide has been the most challenging part of the implementation of the filter. An initial approach led us into the implementation of these walls using lines of via holes in a substrate-integrated waveguide arrangement (Figure IV.5) whose diameter and pitch was calculated according to [5].
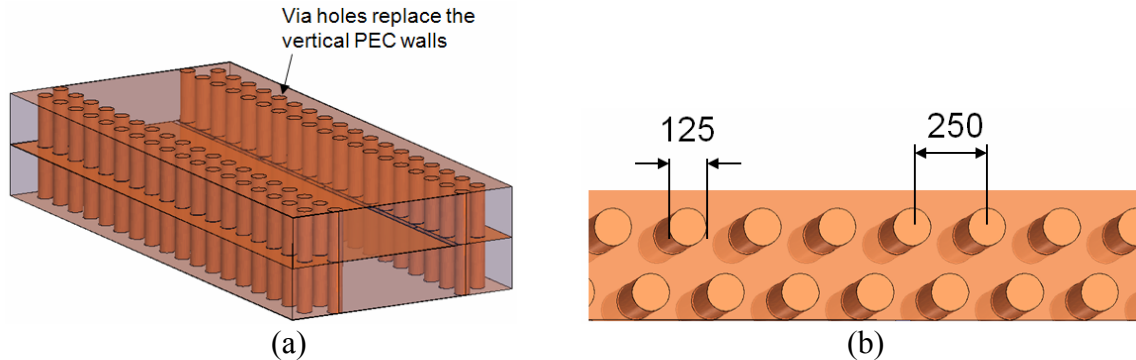
Figure IV.5 - (a) Folded waveguide filter modeled using vertical walls made of via holes in a substrate integrated waveguide fashion, (b) Dimensions of the via wall in μm.

Although simulations showed the successful operation of the filter with the substrate integrated waveguide arrangement, the perforation of such small holes and tight pitch proved to be extremely unfeasible for fabrication. Resonetics LLC (http://www.resonetics.com/), a company that specializes in laser micro machining offered to make perforations for three circuit samples for about $1,950.00 per day of work. However, the company recently communicated to us that they have re-oriented their operation for strictly commercial, large-scale projects which leaves small research projects, such as this project, outside their scope. Other companies have been contacted as well, but none of them have the capability to perform the drilling with such dimensions. Nonetheless, from the design stages it was assumed that the holes would be drilled by Resonetics, so the filter was optimized assuming via-hole walls with the dimensions shown in Figure IV.5.

IV. 5/ Frequency Tuning:

As mentioned previously, frequency tuning is achieved through BST tunable capacitors as demonstrated in [6]. In it is shown [7] that to achieve maximum tuning it is necessary to place the tuning element (in our case the BST capacitor), in the region within each resonating structure where the electric field has maximum intensity. By plotting the electric field distribution in HFSS we can observe that this region is located in the waveguide *slot side* at the middle of each resonator. Thus placing the BST capacitors in the vicinity of region causes the "ideal" tuning presented in Figure IV.7.
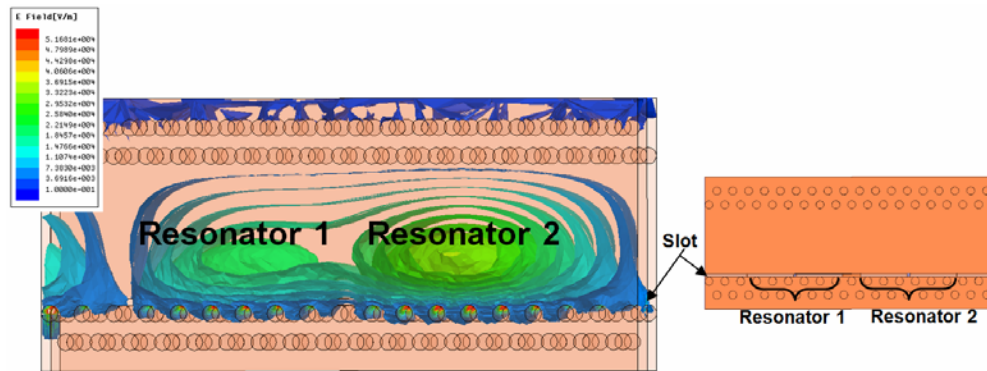
Figure IV.6 - Intensity distribution of the electric field within resonators 1 and 2 of the two-pole folded waveguide filter (top view).

For our simulations in HFSS, the BST capacitors have been modeled as two lumped element sheets: one capacitive and one resistive going from the layout layer (indicated in figure in
Figure IV.4a) towards the vertical walls of the waveguide (ground potential). We can also observe that ideal the insertion loss (IL) has increased to 1.88 dB assuming a resistor value of 1 Ω.

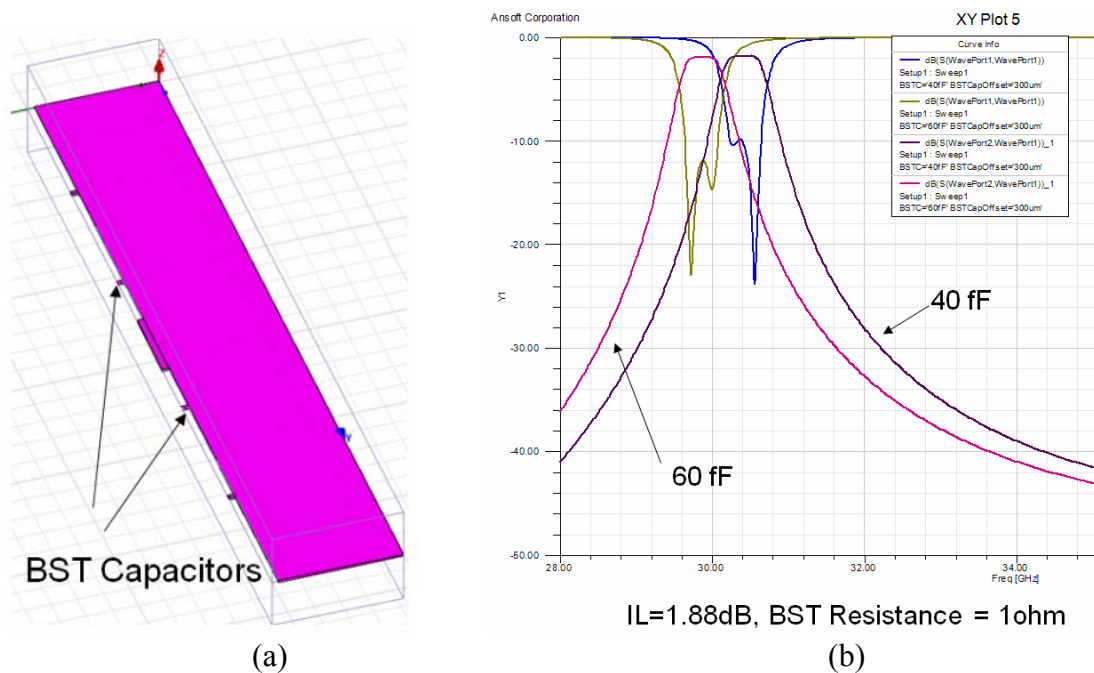(a)   (b)

Figure IV.7 - Two-pole folded waveguide filter with tuning provided by BST capacitors: (a) Ideal model with PEC walls showing BST capacitor placement, (b) Simulated S-parameter response for two capacitance values.

Although placing the tuning element in the region of maximum electric field intensity causes maximum tuning, the fact that our BST capacitors have a significant resistive component has the added disadvantage of causing maximum insertion loss. Thus, a trade-

off is identified in the process of finding the optimal position of the BST capacitor along the folded waveguide slot: insertion loss versus tuning range.

By symmetrically sweeping the position of the capacitors along the slot of the folded waveguide, we see that a 10% tuning and a worse case 5 dB insertion loss is achieved by placing each capacitor at 756 μm from the inter-resonator coupling section. This optimization was performed taking into account the losses introduced by the copper metallization and by an assumed BST capacitor resistance of 10 Ω. A model was also simulated using only one line of via holes to test the effect of the via wall on the insertion loss. Both results are presented in Figure IV.8. A summary of the dimensions of the main features folded waveguide filter is presented in Figure IV.9.
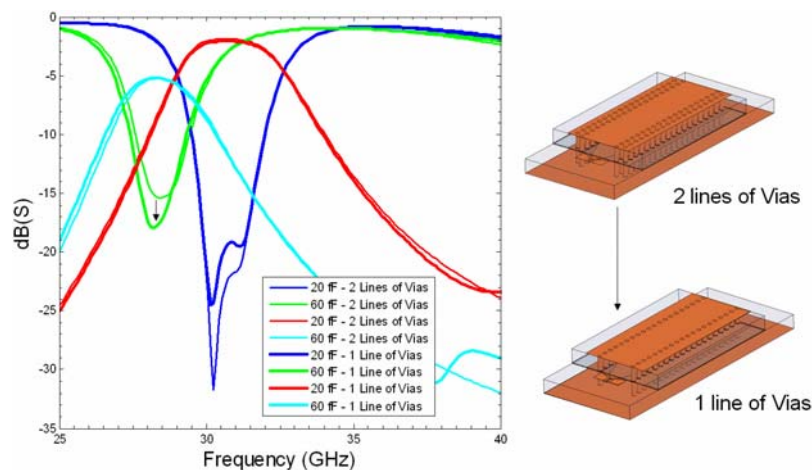

Figure IV.8 - Simulated S-parameter response of the substrate-integrated, folded-waveguide, two-poles filter using one and two lines of via holes as vertical walls.
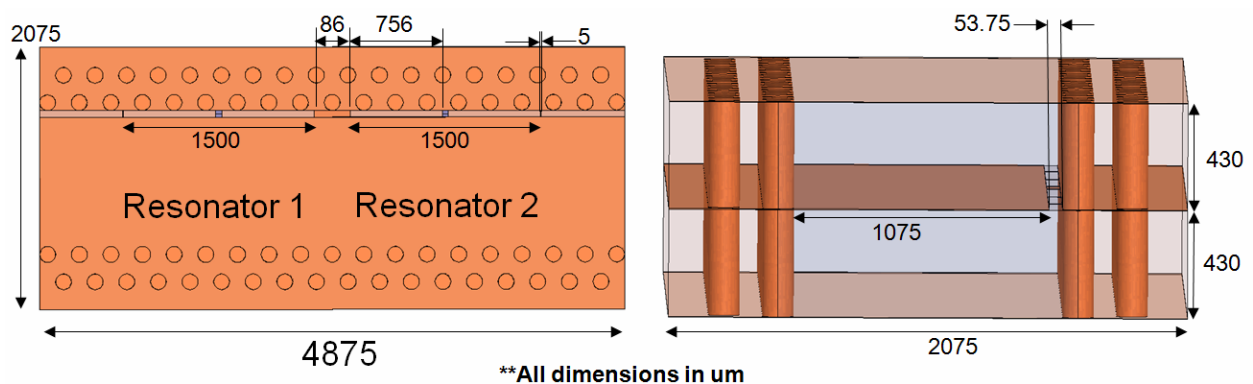

Figure IV.9 - Summary of the optimized dimensions of the two-pole substrate integrated folded waveguide filter in μm.

IV/ 6/ Filter Fabrication:

The fabrication of the folded waveguide filter is performed in a number of stages. First "layout" layer is patterned on the "bottom" sapphire substrate and a layer of cyclotene is applied to provide access to the bias circuitry. Three circuits are patterned in a 10 mm x 10 mm wafer as shown in Figure IV.10.
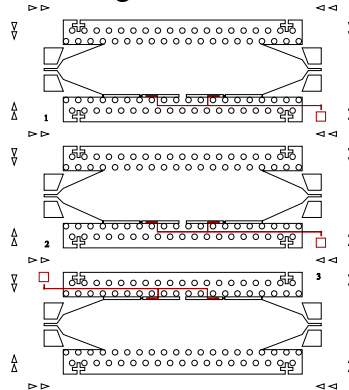

Figure IV.10 - Layout metallization layer patterned on the bottom sapphire layer with BST capacitor lines are shown in red.

Preliminary measurements were performed at this stage of the fabrication to verify the operation of the BST capacitors. Although it is difficult to interpret the measured data, a simulation was performed to study the measured response. The results slight change in the S-parameter response after varying the bias voltage from 0 V to 30 V. A comparison between the measurements and the simulated data (varying the capacitance value from 30 fF to 60 fF) are shown in Figure IV.11.
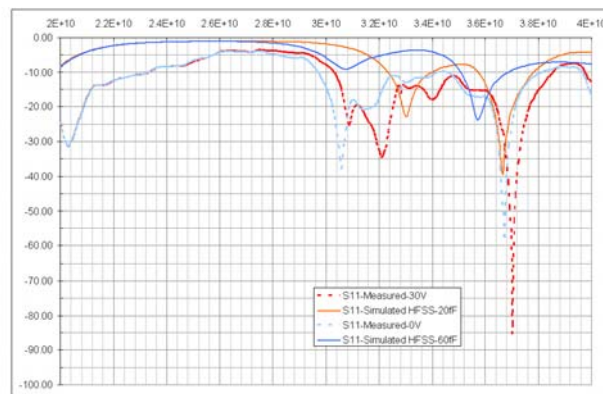
- S11 for Sample UR18C-32-3
- Only with metalization layer over Sapphire and with cyclotene on top.
- Compared to HFSS – Copper Metallization

- S21 for Sample UR18C-32-3
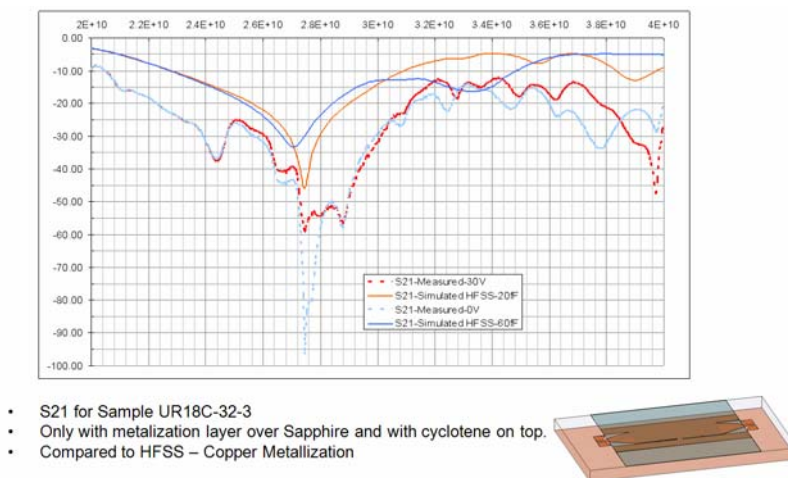- Only with metalization layer over Sapphire and with cyclotene on top.
- Compared to HFSS – Copper Metallization
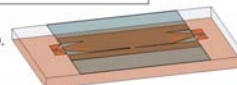
Figure IV.11: Simulated and measured S-parameter response of the metallized bottom sapphire layer.

After the "layout" metallization patterned on the bottom sapphire, the top layer is diced and bonded to the cyclotene using the Rogers 3001 bonding film.   First, the bonding layer is cut using a CO_2 laser system to provide the best accuracy. Then, the bonding is achieved by using a Finetech sub-micron flip-chip bonder. The final substrate stack-up is shown in

Figure IV.12.

Electrical contact between the top-sapphire-layer via holes and the middle metalization layer is crucial to avoid radiation leakage.

Sapphire (430 um, E_r=10, tanD~0.0001)

Rogers 3001 (20 um, E_r=2.28, tanD=0.003)

Cyclotene (7um, E_r=2.65, tanD=0.002)

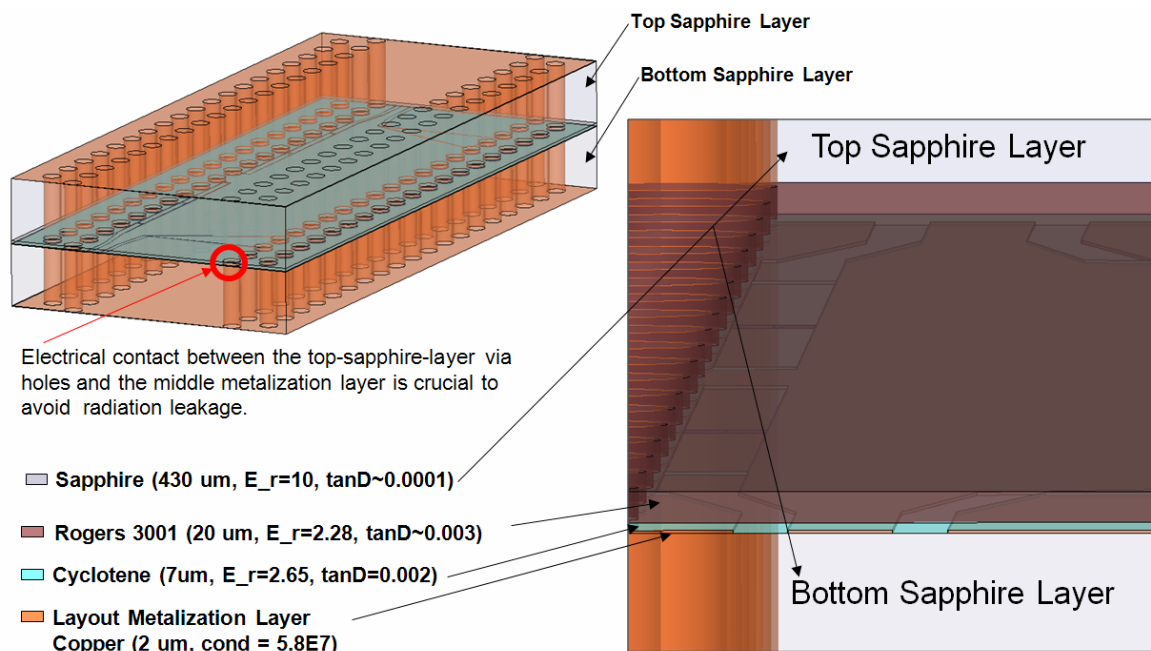Layout Metalization Layer
Copper (2 um, cond = 5.8E7)

Figure IV.12 - Substrate stack-up of the folded-waveguide tunable filter.

Preliminary bonding results performed on dummy samples are shown in Figure IV.13. The estimated misalignment is of about 5-10 µm. This misalignment is caused by the large size of the sample in comparison with the limited movement of the camera used by the alignment system. Another possible source of misalignment is that the alignment marks are seen through the cyclotene in the bottom sapphire layer, which makes it difficult to properly focus the layer for bonding.

Figure IV.13 - Alignment result of bonding the top and bottom sapphire substrate layers (both layers have metallized alignment marks on the bonding side).

IV. 7/ Current status and future work:

Current efforts are focusing in improving the alignment technique for bonding prior to dicing of the individual filters. In addition, studies have been performed to create the vertical walls using solid copper metallization after dicing the samples. With solid vertical walls placed as close as 50 µm to the filter, the simulated filter response is shown in

Figure IV.14. Observe how walls placed at 50 µm from the layout area do not leave room for the BST capacitors bias line in the position it is currently patterned in the fabricated samples.
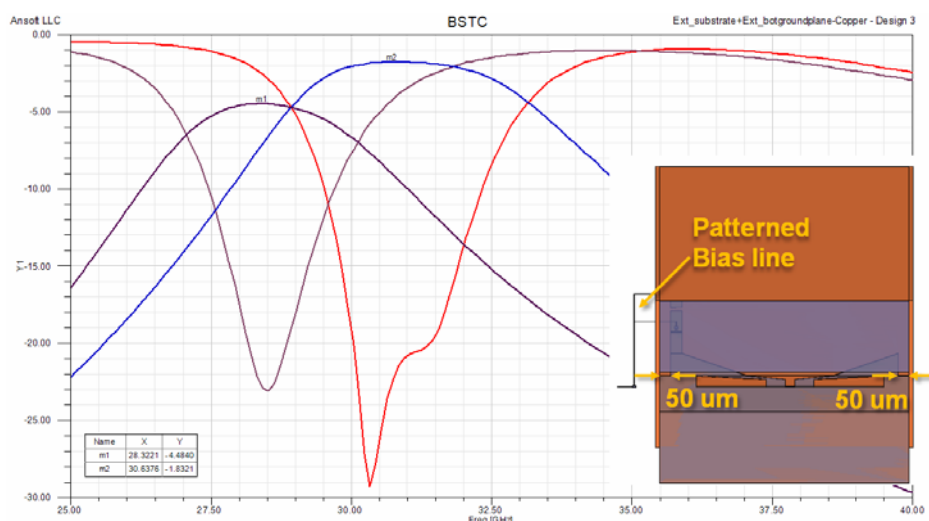
Figure IV.14 - Simulated S-parameter response of the folded waveguide tunable filter
using solid copper for the vertical walls.

Consequently, fabricating vertical walls at 50 μm from the layout area would require a
new fabrication or a test with un-biased BST capacitors. Another option to allow a test to
show tenability would be achieved by providing room for the bias line by extending the
distance to the via-wall. However, the filter response would significantly as observed in
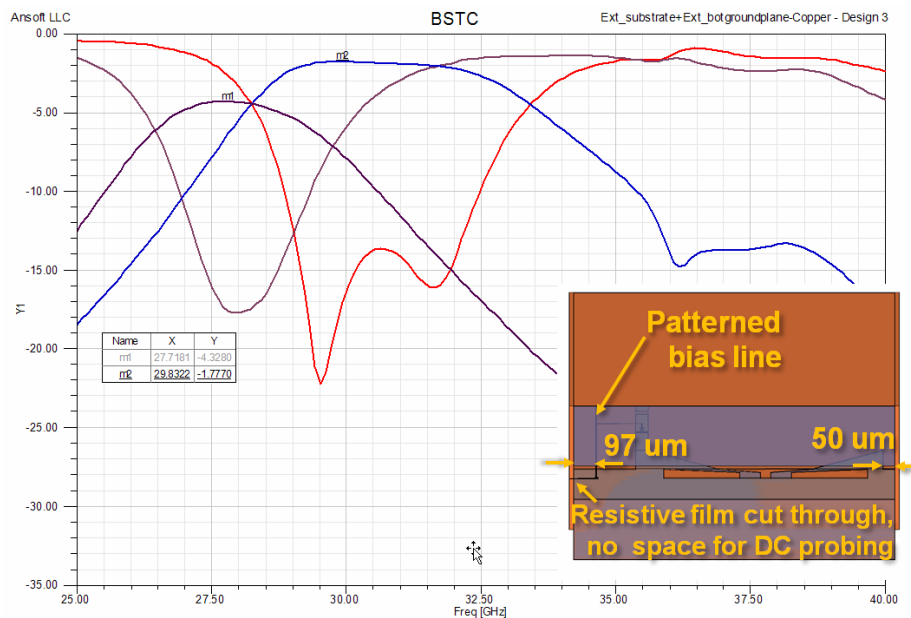Figure IV.15.

Figure IV.15 - Simulated S-parameter response of the tunable folded waveguide filter
extending the distance between the layout area and the vertical wall.

References

[1] N. Grigoropoulos, B. Sanz-Izquierdo, and P. R. Young, "Substrate integrated folded
waveguides (SIFW) and filters", *IEEE Micro. and Wireless Comp. Letters*, vol. 15, no. 12,
pp. 829–831, 2005.

[2] G. H. Zhai, W. Hong, K. Wu, J. X. Chen, P. Chen, and H. J. Tang, "Substrate
integrated folded waveguide (SIFW) narrow-wall directional coupler," in *Proc. Int. Conf.
Microwave and Millimeter Wave Technology ICMMT 2008*, vol. 1, 2008, pp. 174–177.

[3] "High Frequency Structure Simulator (HFSS)," Ansoft LLC, 2009, version 12.0.1.

[4] M. Margraf, S. Jahn, and J. Flucke, "Quite universal circuit simulator (QUCS),"
Available Online at http://qucs.sourceforge.net/, September 2009, version 0.0.15.

[5] K. Wu, D. Deslandes, and Y. Cassivi, "The substrate integrated circuits - a new
concept for high-frequency electronics and optoelectronics," in *Proc. 6th Int. Conf.
Telecommunications in Modern Satellite, Cable and Broadcasting Service TELSIKS 2003*,
vol. 1, 2003.

[6] S. Courrèges, Y. Li, Z. Zhao, K. Choi, A. Hunt, and J. Papapolymerou, "Ferroelectric
tunable bandpass filters for Ka-band applications," in *Proc. 38th European Microwave
Conf. EuMC 2008*, 2008, pp. 55–58.

[7] A. L. Amadjikpe and J. Papapolymerou, "A high-Q electronically tunable evanescent-mode double-ridged rectangular waveguide resonator," in *Proc. IEEE MTT-S Int. Microwave Symp. Digest*, 2008, pp. 1019–1022.

Conclusions:

This report has demonstrated the design and simulations of BST-based tunable bandpass filters that operate in Ka-band.

In the first section, a 3-pole filter is presented. The filter is built on sapphire and uses a coplanar topology. At the highest center frequency, the filter exhibits insertion loss of only 2.5 dB. The maximum bias voltage for the BST is only 30 V. The center frequency tunes from 29 GHz to 34 GHz.

The second section of the report presents a 2-pole filter, also using a coplanar topology. Here, the electrical length of the two resonators can be changed by biasing the BST capacitors, resulting in the tuning of the center frequency. Issues regarding the fabrication have been discussed.

The third section deals with another CPW Ka-band filter. In that case, cross-coupled resonators are used and 4 BST capacitors that are located at the ends of each resonator in order to make the center frequency of the filter tune. The length of the resonators can be adjusted in order to get a better tuning or better performance.

The final section shows the design of a 2-pole tunable folded waveguide filter. The center frequency of this filter can tune from 27.72 GHz to 30.50 GHz. This topology allows a reduction size of 50% compared to standard waveguide filters.

Publications

S. Courrèges, Y. Li, Z. Zhao, K. Choi, A. Hunt, S. Horst, J. D. Cressler, and J. Papapolymerou, "A Ka-Band Electronically Tunable Ferroelectric Filter", *IEEE Micro. and Wireless Comp. Letters*, vol. 19, no. 6, pp. 356-358, 2009.

S. Courrèges, Y. Li, Z. Zhao, K. Choi, A. Hunt, and J. Papapolymerou, "Ferroelectric tunable bandpass filters for Ka-band applications," in *Proc. 38th European Microwave Conf. EuMC 2008*, 2008, pp. 55–58.